GPU-accelerated Stochastic-FDTD Study of Lightning-induced EM Fields over Non-deterministic Terrains

G. G. Pyrialakos[1], **T. T. Zygiridis**[2], **N. V. Kantartzis**[1], **and T. D. Tsiboukis**[1]

[1]Department of Electrical & Computer Engineering, Aristotle University of Thessaloniki, Greece
[2]Department of Informatics & Telecommunications Engineering, University of Western Macedonia, Greece

Abstract— A curvilinear stochastic finite-difference time-domain (S-FDTD) methodology is presented in this paper for the systematic analysis of lightning-induced fields over rough terrains with statistical uncertainties. The novel 3-D technique stems from a covariant/contravariant formulation which can profitably handle the variation of specific parameters during a single run. To achieve further acceleration, graphics processing units (GPUs) with large core densities are utilized, while a set of realistic setups is addressed for the validation of proposed algorithm.

1. INTRODUCTION

A significant number of engineering problems are directly or implicitly related to the electromagnetic (EM) fields generated by lightning strikes. This fact has motivated the development of several schemes for the efficient prediction of such pulses [1–3]. Also, the presence of various uncertainties and especially rough surface/terrain statistical fluctuations, renders these applications an even more challenging area of research [4–6]. To this aim, the multiple-run Monte-Carlo (MC) approach [7] has been a suitable, yet computationally expensive, candidate, while the stochastic finite-difference time-domain (S-FDTD) algorithm [8, 9] and the FDTD-polynomial chaos expansion (FDTD-PCE) technique [10] have been presented as effective alternatives for material and geometric tolerances.

In this paper, a computational framework based on the 3-D FDTD method is presented for uncertainties inherent in certain aspects of lightning-related problems. In particular, the effects that non-flat terrains (altitude varies with respect to the horizontal plane) have on lightning-induced fields are thoroughly investigated. The realistic geometric features are realized via a random rough surface algorithm, where a length-correlation parameter is introduced as an indicator of terrain roughness. To statistically resolve the problem, we first employ the MC technique as a means to extract the stochastic parameters of EM fields. Next, we develop a geometric adaptation of the S-FDTD method along with a modified convolutional perfectly matched layer (CPML), founded on a covariant/contravariant concept, where the statistical variation of suitable curvilinear parameters is considered. Moreover, for the substantial reduction of simulation times, the power of contemporary graphics processing units (GPUs) and optimized parallel programming is exploited. Numerical results from diverse real-world applications reveal the efficiency of the featured technique.

2. DERIVATION OF 3-D GENERALIZED S-FDTD SCHEMES

Assume an arbitrary coordinate system and its g_{pq} $(p, q = 1,\, 2,\, 3)$ metrics, where vectors can be decomposed via the covariant $\mathbf{u}_1$, $\mathbf{u}_2$, $\mathbf{u}_3$ or the contravariant $\mathbf{u}^1$, $\mathbf{u}^2$, $\mathbf{u}^3$ base [11]. In this way, electric $\mathbf{E}$ and magnetic $\mathbf{H}$ field intensities may be analyzed into covariant $(e_1,\, e_2,\, e_3)$, $(h_1,\, h_2,\, h_3)$ or contravariant $(e^1,\, e^2,\, e^3)$, $(h^1,\, h^2,\, h^3)$ components, respectively. Starting with the FDTD expressions, we apply operator $\mathcal{K}$ (mean value M or variance σ^2) to derive the new update equations. For instance, the covariant e_1 electric and the contravariant h^3 magnetic component are written as

$$\begin{aligned}\mathcal{K}\left\{ e_1\big|^{n+1}_{i+\frac{1}{2},j,k}\right\} = \mathcal{K}\Bigg\{ & D_a\big|_{i+\frac{1}{2},j,k}\, e_1\big|^{n}_{i+\frac{1}{2},j,k} + \frac{D_b\big|_{i+\frac{1}{2},j,k}}{\sqrt{g}\Delta u_2}\left(h^3\big|^{n+\frac{1}{2}}_{i+\frac{1}{2},j+\frac{1}{2},k} - h^3\big|^{n+\frac{1}{2}}_{i+\frac{1}{2},j-\frac{1}{2},k} + \zeta_{e_{12}}\big|^{n+\frac{1}{2}}_{i+\frac{1}{2},j,k}\right) \\ & - \frac{D_b\big|_{i+\frac{1}{2},j,k}}{\sqrt{g}\Delta u_3}\left(h^2\big|^{n+\frac{1}{2}}_{i+\frac{1}{2},j,k+\frac{1}{2}} - h^2\big|^{n+\frac{1}{2}}_{i+\frac{1}{2},j,k-\frac{1}{2}} + \zeta_{e_{13}}\big|^{n+\frac{1}{2}}_{i+\frac{1}{2},j,k}\right)\Bigg\}, \end{aligned} \tag{1}$$

$$\begin{aligned} h^3\big|^{n+\frac{1}{2}}_{i+\frac{1}{2},j+\frac{1}{2},k} = {} & g_{33}\, h_3\big|^{n+\frac{1}{2}}_{i+\frac{1}{2},j+\frac{1}{2},k} + \frac{g_{31}}{4}\left(h_1\big|^{n+\frac{1}{2}}_{i+1,j+\frac{1}{2},k+\frac{1}{2}} + h_1\big|^{n+\frac{1}{2}}_{i+1,j+\frac{1}{2},k-\frac{1}{2}} + h_1\big|^{n+\frac{1}{2}}_{i,j+\frac{1}{2},k+\frac{1}{2}} + h_1\big|^{n+\frac{1}{2}}_{i,j+\frac{1}{2},k-\frac{1}{2}}\right) \\ & + \frac{g_{32}}{4}\left(h_2\big|^{n+\frac{1}{2}}_{i+\frac{1}{2},j+1,k+\frac{1}{2}} + h_2\big|^{n+\frac{1}{2}}_{i+\frac{1}{2},j+1,k-\frac{1}{2}} + h_2\big|^{n+\frac{1}{2}}_{i+\frac{1}{2},j,k+\frac{1}{2}} + h_2\big|^{n+\frac{1}{2}}_{i+\frac{1}{2},j,k-\frac{1}{2}}\right), \end{aligned} \tag{2}$$

where g is the Jacobian determinant and Δu_p the spatial step along the covariant u_p direction. Coefficients $D_a|_{i+\frac{1}{2},j,k} = (2\varepsilon_{i+\frac{1}{2},j,k} - \bar{\sigma}_{i+\frac{1}{2},j,k}\Delta t)/(2\varepsilon_{i+\frac{1}{2},j,k} + \bar{\sigma}_{i+\frac{1}{2},j,k}\Delta t)$ and $D_b|_{i+\frac{1}{2},j,k} = 2\Delta t/(2\varepsilon_{i+\frac{1}{2},j,k} + \bar{\sigma}_{i+\frac{1}{2},j,k}\Delta t)$ contain all media parameters, while ζ are the covariant CPML components [12].

Generally, a stochastic variable can be any of the g_{pq} elements of the Jacobian matrix in (1) and (2). However, our interest focuses exclusively on a small stretch on the z axis, along a few cells vertical to the ground surface. So, we introduce a single stochastic variable affecting only two of the metric variables, i.e., g_{33} and $\sqrt{g}$. The next step is to reduce M and σ^2 to the individual variables of both parts. To this goal, we use the Delta method [13], which applies a Taylor series expansion on each side of (1) and (2). Thus, selecting up to first-order approximations [8], the mean value and variance of an $f(x_1, x_2, \ldots, x_n)$ function with multiple random variables $x_1, x_2, \ldots, x_n$, are

$$M\{f(x_1, x_2, \ldots, x_n)\} \approx f(m_{x_1}, m_{x_2}, \ldots, m_{x_n}), \tag{3}$$

$$\sigma^2\{f(x_1, x_2, \ldots, x_n)\} \approx \sum_{i=1}^{n}\sum_{j=1}^{n} \left.\frac{\partial f}{\partial x_i}\frac{\partial f}{\partial x_j}\right|_m M\left\{(x_i - m_{x_i})(x_j - m_{x_j})\right\}, \tag{4}$$

where $m = m_{x_1}, m_{x_2}, \ldots, m_{x_n}$ are the mean values of x_1, x_2, $\ldots$, x_n. We may notice that the mean value calculation reduces to the regular FDTD one, by replacing each random variable with its mean value. In contrast, to calculate the variance, we must set $\mathcal{K} = \sigma^2$ and then take into account the $\sigma^2\{x_1 \pm x_2\} = \sigma^2\{x_1\} + \sigma^2\{x_2\} \pm 2\mathrm{Cov}\{x_1, x_2\}$ relation for all added terms in (1) and (2), after the application of (4), with $\mathrm{Cov}\{x_1, x_2\} = \rho_{x_1,x_2}\sigma\{x_1\}\sigma\{x_2\}$ the covariance of random variables x_1, x_2. Observe that ρ is an indicator of the stochastic dependence between metric variables and EM fields. Nonetheless, having only a single independent stochastic variable (i.e., the vertical stretch) and considering small perturbations for an almost linear relationship, we may safely set $\rho = 1$. In this context, the standard deviation of the contravariant e^1 electric component is given by

$$\begin{aligned}
\sigma\left\{e^1\big|^{n+1}_{i+\frac{1}{2},j,k}\right\} =& \,\sigma\{g_{11}(\varphi)\}\, M\left\{e_1\big|^{n+1}_{i+\frac{1}{2},j,k}\right\} - M\{g_{11}(\varphi)\}\,\sigma\left\{e_1\big|^{n+1}_{i+\frac{1}{2},j,k}\right\} \\
&+\frac{\sigma\{g_{12}(\varphi)\}}{4}\left(M\left\{e_2\big|^{n+1}_{i+1,j+\frac{1}{2},k}\right\}+M\left\{e_2\big|^{n+1}_{i+1,j-\frac{1}{2},k}\right\}+M\left\{e_2\big|^{n+1}_{i,j+\frac{1}{2},k}\right\}+M\left\{e_2\big|^{n+1}_{i,j-\frac{1}{2},k}\right\}\right) \\
&-\frac{M\{g_{12}(\varphi)\}}{4}\left(\sigma\left\{e_2\big|^{n+1}_{i+1,j+\frac{1}{2},k}\right\}+\sigma\left\{e_2\big|^{n+1}_{i+1,j-\frac{1}{2},k}\right\}+\sigma\left\{e_2\big|^{n+1}_{i,j+\frac{1}{2},k}\right\}+\sigma\left\{e_2\big|^{n+1}_{i,j-\frac{1}{2},k}\right\}\right) \\
&+\frac{\sigma\{g_{13}(\varphi)\}}{4}\left(M\left\{e_3\big|^{n+1}_{i+1,j,k+\frac{1}{2}}\right\}+M\left\{e_3\big|^{n+1}_{i+1,j,k-\frac{1}{2}}\right\}+M\left\{e_3\big|^{n+1}_{i,j,k+\frac{1}{2}}\right\}+M\left\{e_3\big|^{n+1}_{i,j,k-\frac{1}{2}}\right\}\right) \\
&-\frac{M\{g_{13}(\varphi)\}}{4}\left(\sigma\left\{e_3\big|^{n+1}_{i+1,j,k+\frac{1}{2}}\right\}+\sigma\left\{e_3\big|^{n+1}_{i+1,j,k-\frac{1}{2}}\right\}+\sigma\left\{e_3\big|^{n+1}_{i,j,k+\frac{1}{2}}\right\}+\sigma\left\{e_3\big|^{n+1}_{i,j,k-\frac{1}{2}}\right\}\right),
\end{aligned} \tag{5}$$

with analogous equations formed for the other EM quantities. It is stressed that the incorporation of the above geometric uncertainties does not influence the discretization procedure of our algorithm, hence permitting the consistent manipulation of more arbitrary geometries.

3. ACCELARATION VIA GPU AND CUDA PROGRAMMING

The proposed algorithm has been developed via the CUDA 6.0 (compute unified device architecture) programming platform to exploit the capabilities of modern multiprocessor GPUs. This choice is additionally favored by the parallelization potential of the FDTD method [14, 15]. The nature of the technique allows the fully independent execution of update equations at each point in the domain at a single time-step. Based on this remark, we assign each point of our computational space to the various independent execution flows of the hardware, in an attempt to achieve the maximum performance through a thorough optimization process. In the CUDA programming environment, independent processes (threads) are arranged in an algorithmic 3-D "grid". Such a structure provides these threads with unique coordinates, hence allowing the manipulation of the actual space coordinates in the domain. To accomplish this objective, we assign specific memory addresses from our 3-D matrix (i.e., the EM field space) to specific thread coordinates, for the entire simulation space, and simultaneously connect nearby memory addresses with equally adjacent threads.

Several optimization strategies have been hitherto employed to offer a better performance. For a high degree of parallelization, the kernels have been optimized in terms of the block size. A grouping of 32×16 threads-per-block guarantees very good performance, with a measured difference of over 20% in simulation time, compared to other block-size options. In the simple case of fully orthogonal grids for the update of each field, such a task seems sufficient. However, we have found that a multi-kernel implementation is more beneficial for our S-FDTD algorithm. To calculate fields in the absorbing layers, 2 groups of kernels are introduced. Each one comprises 12 extra CPML kernels and is initiated after the execution of the corresponding main ones. This structure is the result of our pursuit for optimal performance, which determined that each kernel should be responsible for one boundary layer as well as for a specific component of the EM field. Specifically, the update process within each of the domain's 6 sides requires 4 different kernels (2 for electric and 2 for magnetic components) in order for the necessary additional calculations (due to the extra CPML terms) to be completed. Also, to increase parallelization, we use streams since they allow kernels to be executed concurrently. Thanks to them, we have been able to partially achieve the simultaneous execution of the main and the CPML kernels. The increase in performance reaches up to 30%, however this usually declines as the number of cells in the FDTD grid rises.

Finally, various types of memories available in the hardware have been utilized, including the global memory for the storage of the main field components and CPML variables, along with the constant memory for storing the constants used in each simulation. Parameter matrices are also loaded to global memory, yet mapped to a surface reference, exploiting the texture memory. Attention has been drawn to the proper matrix alignment in memory, which ensures that adjacent threads in the kernels access similarly-placed elements from memory. Only when the prior action takes place, then transfers of 32 elements from global memory (in the case of floats) are performed in a single access cycle (coalesced access), decreasing by over half the time for a kernel cycle.

4. CONFIGURATION OF THE NON-DETERMINISTIC TERRAIN PROBLEM

The application of the featured methodology concentrates on the analysis of lightning-oriented EM fields in the vicinity of a non-deterministic terrain, whose specific structural variables are known and enable us to perform realistic time-wise stochastic simulations. For this purpose, we introduce the mean height of the altitude Mh along with a correlation length coefficient cl, as indicators of horizontal diversity, either assumed predetermined or varying within a small fluctuation width. Typical Mh values will not exceed the level of 1 or 2 meters, which may cause accuracy issues with the selected Yee cell of $1\,\mathrm{m}^3$ volume, owing to poor staircase approximation in standard meshes. So, we exploit the aforementioned curvilinear S-FDTD algorithm to decrease the cell height in the problematic regions (Figure 1(a)), without sacrificing valuable resources elsewhere in the grid.

To generate the desired terrain, we apply the random rough surface (RRS) algorithm [13]. The power spectral density function is defined as a 2-D uniform pulse bounded by the prefixed cl values. Assuming a Gaussian distribution of the power for each spatial frequency, we conduct the convolution with the analytically calculated inverse Fourier transform of the defined density function. Figure 1(b) presents some indicative ground structures, obtained through this process. Moreover, all field quantities are computed in a 3-D space, occupied by either air or ground with $\varepsilon = 5\varepsilon_0$ and a conductivity of $\bar{\sigma} = 0.01\,\mathrm{S/m}$. The excitation sources appear only in the lightning channel, where the current distribution is described by $I(z,t) = I(0, t - z/v)e^{-\alpha z}u(t - z/v)$, with $u(t)$ the unit-step function, $v = 1.5 \times 10^8\,\mathrm{m/s}$ the speed of the return stroke, $\alpha = 1/2000\,\mathrm{m}^{-1}$ the exponential decay, and $I(0,t)$ the temporal variation of the channel base current expressed as

$$I(0,t) = \sum_{\ell=1}^{2} \frac{I_{0\ell}}{\eta_\ell} \left(\frac{t}{\tau_{\ell 1}}\right)^2 \frac{e^{-t/\tau_{\ell 2}}}{1 + (t/\tau_{\ell 1})^2} \quad \text{for} \quad \eta_\ell = \exp\left[-(\tau_{\ell 1}/\tau_{\ell 2})\sqrt{(2\tau_{\ell 2}/\tau_{\ell 1})}\right], \tag{6}$$

and $\ell = 1, 2$. The remaining parameters in (6) receive the typical values for the subsequent

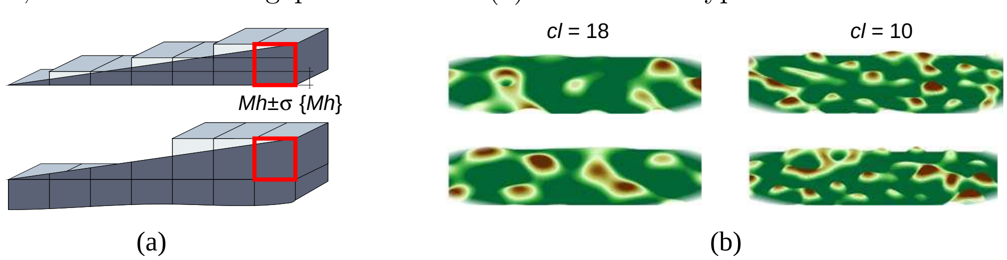

Figure 1: (a) Staircase optimization via a non-square grid at the ground-air interface (red rectangle indicates the problematic (lower) and the optimized (upper) area) and (b) a variety of stochastic ground structures.

stroke, i.e., $I_{01} = 10.7\,\mathrm{kA}$, $\tau_{11} = 0.25\,\mu\mathrm{s}$, $\tau_{12} = 2.5\,\mu\mathrm{s}$ and $I_{02} = 6.5\,\mathrm{kA}$, $\tau_{21} = 2\,\mu\mathrm{s}$, $\tau_{11} = 230\,\mu\mathrm{s}$. With z referring to the height of ground's surface, the computational domain is discretized into $150 \times 150 \times 1000$ cells and truncated by a 16-cell CPML with a quadratic conductivity profile.

5. NUMERICAL VERIFICATION

The first scenario deals with the extraction of statistical results for the lighting-induced fields, taking into account the lack of knowledge for the exact terrain profile. Through a MC approach, and choosing a constant cl parameter, we obtain the numerical outcomes of Figure 2. Three different cl values are depicted for both the mean value and standard deviation of the radial electric field component, 100 m away from the source. It can be detected that the standard deviation of the field values is quite significant and may reach some levels up to the 10% of the mean value at the corresponding time instants. In addition, one may deduce that larger correlation lengths trigger higher field levels. Such an observation is to be expected, since shorter correlation lengths imply "rougher" surfaces which create a stronger scattering from the ground at random directions.

In the second application, we select a specific terrain shape, generated from the RRS algorithm and embedded in the geometry for every simulation. The variation is then induced at the height of the surface by perturbing the associated metric variables on a $150\,\mathrm{m} \times 50\,\mathrm{m} \times 10\,\mathrm{m}$ section of the computational mesh that includes the air-ground interface. The retrieval of the mean value and variance is performed via both the MC and the curvilinear S-FDTD method, while results are given in Figures 3(a) and 3(b) for the radial electric field component at the same point as in the previous example and a height variance of $\sigma\{Mh\} = 0.01Mh$. A very good agreement is achieved, justifying the competence of the novel method to provide accurate stochastic simulations. Nevertheless, compared to the above case, one may notice significantly lower values for the standard deviation.

For a more comprehensive and real-world examination of the effects of a random terrain environment, we consider both the height and shape of the terrain in a single MC simulation. At each run, we generate a different terrain with a constant cl and perform an S-FDTD simulation; therefore automatically involving the height variance. It is clarified, herein, that such an approach is the only efficient way of extracting the desired results. A full MC solution would inevitably

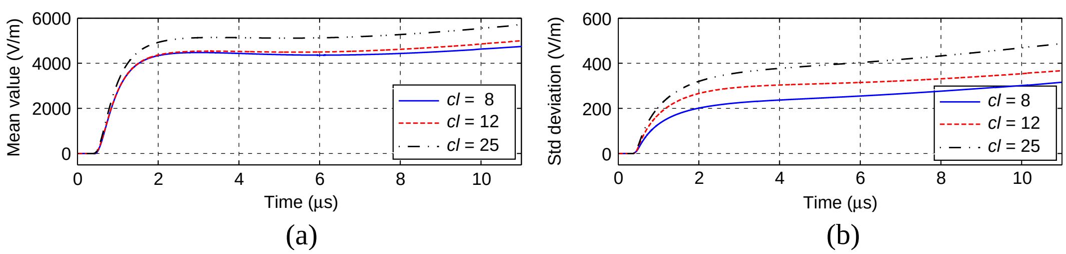

Figure 2: (a) Mean value and (b) standard deviation of the radial electric field, obtained with MC simulations, at point $(r, z) = (100\,\mathrm{m}, 10\,\mathrm{m})$, in the case of a non-flat terrain.

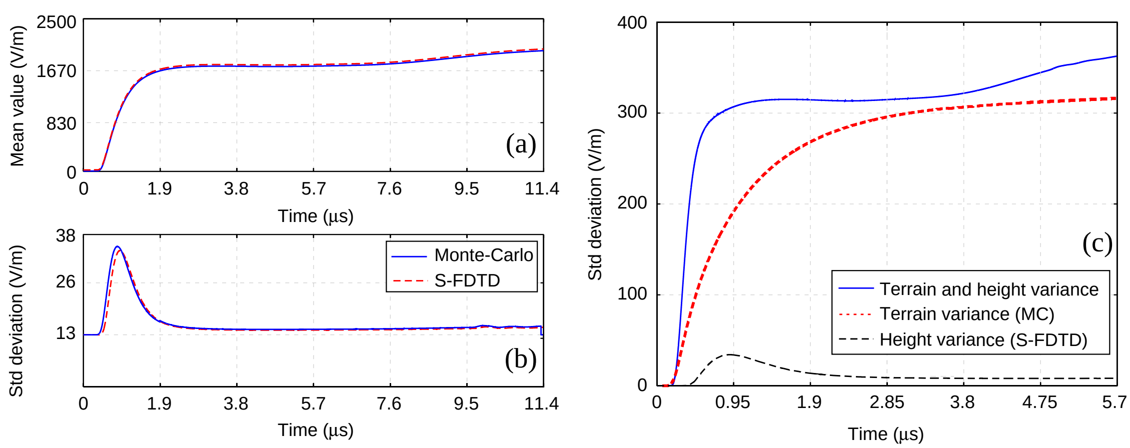

Figure 3: (a) Mean value and (b) standard deviation of the radial electric field for a specific terrain shape, when $\sigma\{Mh\} = 0.01Mh$. (c) Standard deviation when both the terrain shape and height are considered.

involve several other FDTD runs to account for the height, requiring excessive simulation times, even with an optimized CUDA implementation. Figure 3(c) illustrates the final results for $cl = 12$ and $\sigma\{Mh\} = 0.01Mh$ together with a curve extracted from a single S-FDTD run, whereas the corresponding curve from Figure 1(b), for the specific parameters, is also repeated for comparison. It becomes evident that the morphology of the terrain, rather than its height, has the most profound effect on the field variance. Finally, it should be mentioned that in all simulations the use of GPU achieved up to 50 times decrease in execution time both for the featured S-FDTD and MC method.

6. CONCLUSION

The accurate modeling of lightning-generated EM fields over arbitrarily-rough terrains with non-deterministic geometric variations has been conducted in this paper, through a 3-D GPU-accelerated S-FDTD algorithm. The new single-run method is based on a consistent covariant/contravariant formulation, blended with a properly altered CPML. Numerical outcomes prove the reliability of the technique along with its enhanced speed, unlike the overall time required by existing approaches.

ACKNOWLEDGMENT

This research has been co-financed by the EU and Greek national funds through the Operational Program "Education and Lifelong Learning" of the NSRF — Research Funding Program: Aristeia.

REFERENCES

1. Khosravi-Fasrani, M., R. Moini, S. H. H. Sadeghi, and F. Rachidi, "On the validity of approximate formulas for the evaluation of the lightning electromagnetic fields in the presence of a lossy ground," *IEEE Trans. Electromagn. Compat.*, Vol. 55, No. 2, 362–370, 2013.
2. Baba, Y. and V. A. Rakov, "Applications of the FDTD method to lightning EM pulse and surge simulations," *IEEE Trans. Electromagn. Compat.*, Vol. 56, No. 6, 1506–1521, 2014.
3. Izadi, M., M. Z. A. Ab Kadir, and C. Gomes, "Evaluation of electromagnetic fields associated with inclined lightning channel using second order FDTD-hybrid methods," *Progress In Electromagnetics Research*, Vol. 117, 209–236, 2011.
4. Zhang, Q., J. Yang, X. Jing, D. Li, and Z. Wang, "Propagation effect of a fractal rough ground on the lightning-radiated vertical electric field," *Atmos. Res.*, Vols. 104–105, 202–208, 2012.
5. Shoory, A., A. Mimouni, F. Rachidi, V. Cooray, R. Moini, and S. H. H. Sadeghi, "Validity of simplified approaches for the evaluation of lightning electromagnetic fields above a horizontally stratified ground," *IEEE Trans. Electromagn. Compat.*, Vol. 52, No. 3, 657–663, 2010.
6. Li, D., Q. Zhang, Z. Wang, and T. Liu, "Computation of lightning horizontal field over the two-dimensional rough ground by using the three-dimensional FDTD," *IEEE Trans. Electromagn. Compat.*, Vol. 56, No. 1, 143–148, 2014.
7. Hastings, F. D., J. B. Schneider, and S. L. Broschat, "A Monte-Carlo FDTD technique for rough surface scattering," *IEEE Trans. Antennas Propag.*, Vol. 43, No. 11, 1183–1191, 1995.
8. Smith, S. M. and C. Furse, "Stochastic FDTD for analysis of statistical variation in electromagnetic fields," *IEEE Trans. Antennas Propag.*, Vol. 60, No. 7, 3343–3350, 2012.
9. Tan, T., A. Taflove, and V. Backman, "Single realization stochastic FDTD for weak scattering waves in random media," *IEEE Trans. Antennas Propag.*, Vol. 61, No. 2, 818–828, 2013.
10. Austin, A. C. M. and C. D. Sarris, "Efficient analysis of geometrical uncertainty in the FDTD method using polynomial chaos with application to microwave circuits," *IEEE Trans. Microw. Theory Tech.*, Vol. 61, No. 12, 4293–4301, 2013.
11. Taflove, A. and S. C. Hagness, *Computational Electrodynamics: The Finite-difference Time-domain Method*, Artech House, Boston, 2005.
12. Roden, J. A. and S. D. Gedney, "Convolution PML (CPML): An FDTD implementation of the CFS-PML for arbitrary media," *Microw. Opt. Technol. Lett.*, Vol. 27, No. 5, 334–339, 2000.
13. Le Maitre, O. and O. Knio, *Spectral Methods for Uncertainty Quantification with Applications to Computational Fluid Dynamics*, Springer-Verlag, Heidelberg, 2010.
14. De Donno, D., A. Esposito, L. Tarricone, and L. Catarinucci, "Introduction to GPU computing and CUDA programming: A case study on FDTD [EM programmers notebook]," *IEEE Antennas Propag. Mag.*, Vol. 52, No. 3, 116–122, 2010.
15. Wahl, P., D. S. Ly Gagnon, C. Debaes, J. Van Erps, N. Vermeulen, D. A. B. Miller, and H. Thienpont, "B-Calm: An open-source multi-Gpu-based 3D-FDTD with multi-pole dispersion for plasmonics," *Progress In Electromagnetics Research*, Vol. 138, 467–478, 2013.